Bidimensional intercalation of Ge between SiC(0001) and a heteroepitaxial graphite top layer

L. Kubler,[1,*] K. Aït-Mansour,[2] M. Diani,[3] D. Dentel,[1] J.-L. Bischoff,[1] and M. Derivaz[1]
[1]*LPSE, UMR CNRS-7014, Faculté des Sciences, 4, rue des Frères Lumière, 68093 Mulhouse Cedex, France*
[2]*Materials Testing and Research (EMPA), Feuerwerkerstrasse 39, 3602 Thun, Switzerland*
[3]*LSGM, Département de Physique, Faculté des Sciences et Techniques, BP 416, Tanger, Morocco*
(Received 14 March 2005; revised manuscript received 18 May 2005; published 16 September 2005)

High temperature annealing of 4H- or 6H-SiC(0001) crystals is well known to desorb Si from the surface and to generate a C-rich $(6\sqrt{3}\times 6\sqrt{3})$R30° $(6\sqrt{3})$ reconstruction explained as a graphite monolayer in heteroepitaxial registry with the substrate. Ge deposition at room temperature and in the monolayer range on this graphitized reconstruction results in Ge islands. Using a number of surface techniques, we follow subsequent Ge morphology evolutions as a function of isochronal post-annealing treatments at increasing temperatures. In a particular temperature window Ge reacts with the substrate by diffusion under the graphite planes and wets the Si-terminated SiC surface. In spite of this bidimensional insertion of a Ge layer, the epitaxial relationship between the SiC substrate and the graphite is maintained as shown by very clear graphite-(1×1) LEED or RHEED patterns. They denote extended and well-ordered graphite planes at the surface of a graphite/Ge/SiC heterostructure. XPS analyses reveal a complete passivation of the intercalated Ge layer against oxidation by the overlying graphite sheets. Moreover, drastic spectroscopic changes on the bulk-SiC Si $2p$ and C $1s$ core levels are observed, depending on whether graphite$(6\sqrt{3})$/SiC or graphite(1×1)/Ge/SiC terminations are analyzed. In the latter case, the observed core level splitting of the bulk components is interpreted by a significant upward band bending (~1.2 eV) of the n-doped SiC, making this second interface to act as a Schottky barrier. Above 1300 °C, a delayed Ge desorption takes place that allows the graphite sheets to re-form in their initial $6\sqrt{3}$ form, i.e., without Ge and with flatter bands.

DOI: 10.1103/PhysRevB.72.115319 PACS number(s): 68.55.−a, 79.60.Jv, 61.14.−x

I. INTRODUCTION

Longstanding studies have characterized C-enriched SiC(0001) surfaces and their relevant $(6\sqrt{3}\times 6\sqrt{3})$R30° $(6\sqrt{3})$ reconstruction as a monocrystalline graphite overlayer, azimuthally oriented on the SiC(0001) surface.[1–9] The question is nevertheless still open to know whether the graphite top layer is floating directly above a bulk truncated and ideally Si-terminated SiC(0001) face[1,2,9] or on a $\sqrt{3}\times\sqrt{3}$R30° $(\sqrt{3})$-reconstructed Si-rich surface.[3,6–8] The Si adatoms in T_4 positions of the latter $\sqrt{3}$ reconstruction[3] would contribute to anchor the graphite planes[6–8] in specific azimuth orientations of the SiC surface. It is noteworthy that the graphite unit cell must be rotated by 30° with respect to the SiC one to explain the $6\sqrt{3}$ reconstruction.[1–3,6,8,9] Such a situation would imply an easy intercalation of additional atoms in the rather wide space (about 4.5 Å)[7] between the substrate and the overlying and weakly bond graphite planes. The door may thus be opened to the elaboration on SiC substrates of stable, semiconducting 2D δ layers, passivated by the graphite capping planes.

In order to explore possibilities to fabricate quantum dots with large band gap offsets, more or less systematic Ge growth studies have recently been conducted on the different surface terminations of 4H or 6H-SiC.[10–19] These studies have pointed out general 3D growth modes,[15,17–19] except for low Ge coverages [~1 monolayer (ML)] on Si-rich 3×3 and $\sqrt{3}$ surfaces where a wetting 2D Ge-growth may take place in the form of a Ge−4×4 reconstruction.[15–17] On the graphitized $6\sqrt{3}$ surface,[15,17–19] Ge islands are obtained whatever coverages and deposition temperatures denoting the absence of any Ge wetting-layer on the $6\sqrt{3}$-associated graphite planes. This result is already valid for deposition temperatures as low as the room temperature (RT). More or less achieved epitaxy-relationships of these Ge islands are nevertheless obtained depending on the growth temperature.[15–19]

The present study is devoted to report on very particular and surprising growth schemes on the $6\sqrt{3}$ surface when a few Ge monolayers (3 ML) are deposited at RT on the graphitized SiC surface and subjected to a particular thermal treatment consisting in progressive isochronal postannealing steps at increasing temperatures. We intend to show that such thermal treatments induce spectacular and connected morphology changes on both Ge deposit and graphite sheets. At 600 °C, the Ge islands, initially formed by the nonwetting upon the $6\sqrt{3}$ surface, begin to be dismantled. The Ge atoms diffusing towards the underlying SiC surface also dismantle the graphite sheets. Between 700 and 1000 °C, an unusual 3D–2D transition has taken place for Ge, with a final situation where about 1 ML of Ge is now wetting the SiC substrate and minimizing the surface energy. After this transitory stage of Ge subsurface diffusion where very rough graphite morphologies are observed, the graphite sheets reform bidimensionally and ordered over the Ge layer. It should be noticed that graphite returns to an epitaxial relationship with the SiC substrate in spite of the Ge insertion between the SiC and the graphite planes. Indeed, extended graphite-1×1 ordered-areas are replacing the initial $6\sqrt{3}$ reconstruction. Further annealing at temperatures above 1300 °C finally ends in a complete but delayed Ge desorption that allows the graphite sheets to be restored in their initial $6\sqrt{3}$ form. These findings are backed by systematic investigations using *in situ*

reflection high energy electron diffraction (RHEED) and low energy electron diffraction (LEED), X-ray photoelectron spectroscopy (XPS), and X-ray photoelectron diffraction (XPD) measurements and *ex situ* atomic force microscopy (AFM) morphology characterizations.

II. EXPERIMENT

In situ substrate surface preparations and depositions are carried out in an ultrahigh vacuum (UHV) (10^{-10} mbar) molecular beam epitaxy (MBE) chamber of the LPSE (Mulhouse), using Knudsen effusion cells for Ge or Si evaporations. This chamber is equipped with a RHEED system, operating at an accelerating voltage of 30 kV. A charge coupled device camera, connected to a STAIB-Vision software, allows a real-time crystallographic characterization of the surface. RHEED patterns are recorded in [1–100]–SiC azimuths with electron beams at glancing incidence angles of about 1°. A second UHV chamber, coupled to the first one, is equipped with LEED and XPS, the latter technique allowing chemical characterizations. Conventional Mg $K\alpha$ (1253.6 eV) and Al $K\alpha$ (1486.6 eV) photon sources of a VG CLAM-100 spectrometer are used for photoemission spectra acquisition. The studies are performed on Si-terminated faces of on-axis 4H-SiC monocrystals, purchased from Cree, Inc. XPS analyses of the as-received samples showed significant Zn impurity amounts at the surface, probably due to the final sample slicing. The substrates are therefore subjected to an *ex situ* chemical treatment by an acid solution (70% H_2SO_4+30% H_2O_2). The resulting (0001) faces, showing SiC–1×1 RHEED and LEED diagrams, mainly due to oxygen contamination, are then *in situ* cleaned. The native oxide desorbs at 850 °C using a weak MBE atomic Si flux (around 1 ML/min, controlled by a quartz microbalance) during 5 min. One ML is defined to be the ideal Si atom density in an SiC(0001) plane, i.e., 1.22×10^{15} atoms/cm^2. As controlled by RHEED, LEED, and XPS, such cleaning procedures result in clear and well-ordered 3×3 reconstructed surfaces.[6–9,15–19] *Ex situ* AFM images in the tapping mode allow us to observe rather large (0.6 μm) and flat terraces separated by steps of different heights, all multiples of about 5 Å, a value close to the thickness of two SiC bi-layers or half the c-parameter of 4H-SiC (10.1 Å).[16,18]

The other stable $6\sqrt{3}$ reconstruction is obtained by further extensive heating at higher temperatures (around 30 min at 1250 °C), without Si flux. The 3×3 Si excess is thus progressively depleted (see Refs. 6 and 9, and references therein) and the graphite sheets are formed. As a consequence of this depletion, the surface morphology shown by AFM appears now somewhat rougher, the preceding terraces being now delimited by more steps of increasing heights.

Three ML of Ge are deposited at RT on the $6\sqrt{3}$-reconstructed surface at a growth rate of 1/3 ML/min and are then submitted to a set of isochronal heating (2 min) from 200 to 1350 °C, a temperature leading to a complete Ge desorption from the surface. At each step, a full set of surface analyses are performed, by both RHEED (30 keV) and LEED (100 eV) monitoring, and Si–, C–, and Ge–related XPS core level recording, allowing the control of any temperature induced, structural and chemical surface modifications, respectively. The Ge and graphite morphology evolutions are also checked at some particular temperatures by *ex situ* AFM analysis on separately prepared samples.

III. RESULTS

A. Electron diffractions

Figure 1 synthesizes the structural evolutions taking place for a 3 ML Ge deposit during the whole thermal treatment, as seen by RHEED (a)–(j) and LEED (a′)–(j′). Starting from the well-known $6\sqrt{3}$ signatures[9,15,17–19] of the initial surface (a),(a′), the diagrams after the Ge deposit at RT (b),(b′) become now very faint with a weak persistence of the $6\sqrt{3}$ LEED spots (b′) and no RHEED Ge-related spots (b). The preservation of weak $6\sqrt{3}$ areas (b′) indicates an initial inhomogeneous coverage of rather smooth and unstructured Ge islands or patches. Heating the sample at 200–400 °C does not induce significant structural changes. As a consequence, we do not display corresponding RHEED and LEED patterns. After heating at 500 °C, the Ge islands begin to be structured, as ascertained by the appearance of rings (c) related to relaxed Ge and denoting a poor polycrystalline ordering[15]of the different islands with the substrate. The restoration of a clearer $6\sqrt{3}$ LEED pattern (c′) also indicates a now weaker surface area occupied by these islands that do not greatly perturb the graphite-plane organization. Very drastic morphology changes occur nevertheless after annealing at 600 °C and continue in the 600–800 °C temperature range. The RHEED patterns (d)–(f) now exhibit plenty of bright spots, part of them progressively replacing the Ge-associated rings. As clearly demonstrated in previous studies[15,17–19] and recalled in Fig. 2, this part of spots is attributed to the transmission features of relaxed Ge islands growing in a Volmer-Weber mode and in epitaxial relationship with the SiC substrate. But the complex spot pattern can by no means be reduced to these Ge-features alone. The interspot distances in the reciprocal space of another family of spots is compatible with vertical graphite planes [Fig. 2(b)] probably due to the dismantling of the horizontal graphite planes that "swell" and form still undetermined graphitic 3D nanostructures (onions or nanotubes?) under the influence of the Ge diffusion. A lattice parameter of 3.32 (±0.05) Å may indeed be deduced from these spot distances in good agreement with a (002) lattice plane distance of graphite (3.35 Å). Horizontal graphite planes are therefore reorganized with the rapid emergence after 600 °C of graphite-related 3D morphologies showing vertical planes in addition to the Ge islands. The vision of drastic morphology modifications in this temperature domain will be clearly confirmed by AFM images in real space [Sec. III B]. In the same temperature range, the LEED patterns, more sensitive to the persisting 2D areas than to the preceding 3D morphologies, reveal a progressive disappearance of the initial $6\sqrt{3}$ reconstruction [Fig. 1(d′),(e′)], in line with the previous morphology changes. This reconstruction is replaced by very faint 1×1–SiC spots and by 1×1-graphite features in registry

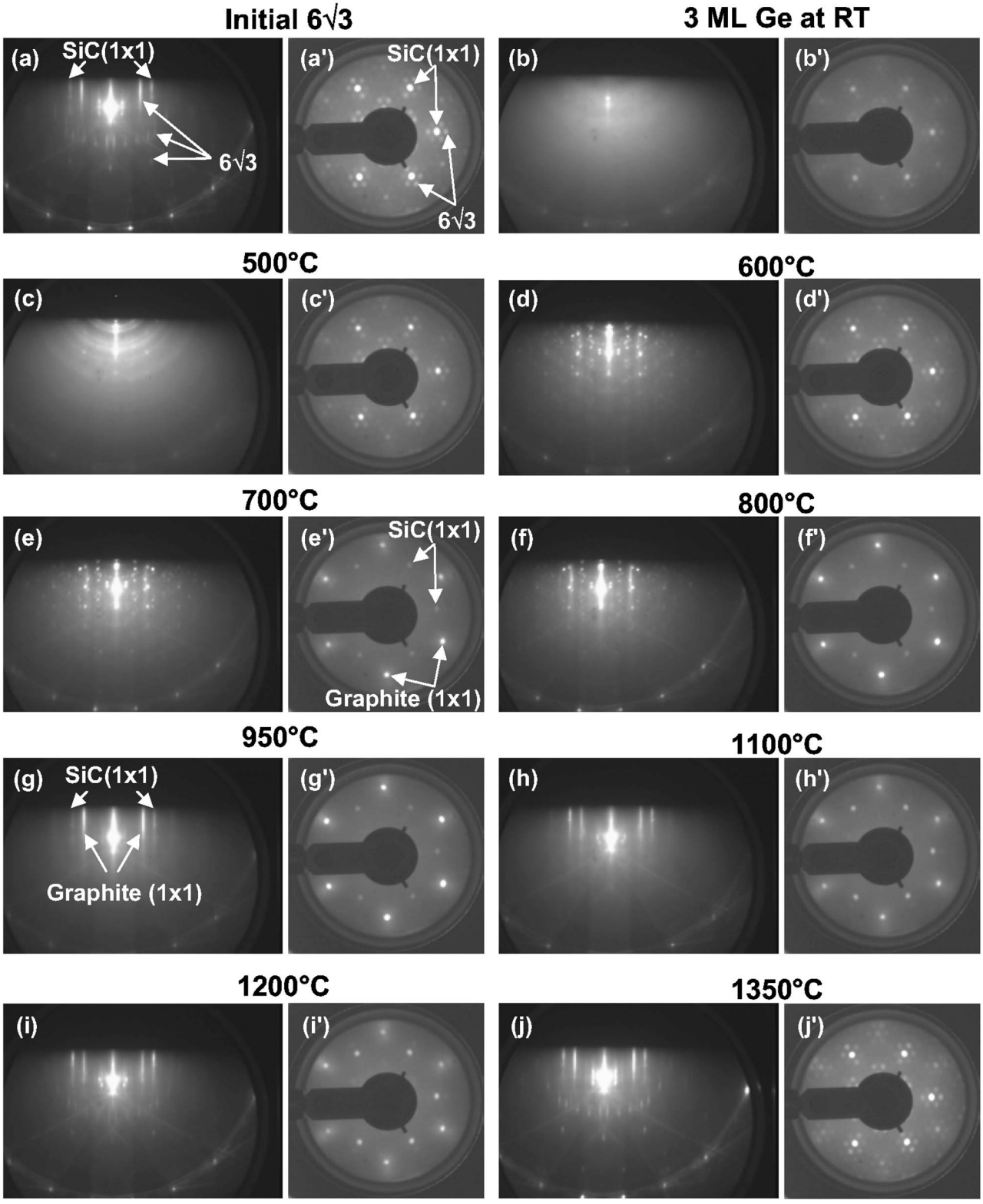

FIG. 1. Typical RHEED (30 keV and [1–100] azimuth) (a)–(j) and LEED (100 eV) (a′)–(j′) patterns of an initial $6\sqrt{3}$ graphitized SiC surface (a),(a′) covered at RT by 3 Ge ML (b),(b′) and after 2 min post-annealing at the indicated temperatures (c)–(j) and (c′)–(j′), respectively.

with the underlying substrate (e′),(f′). From 700 °C, the progressive restoration of bidimensional graphite planes parallel to the surface is confirmed by the reappearance of streaky RHEED patterns (g),(h), also of 1×1-graphite and 1×1–SiC rods. They prove a bidimensional and epitaxial reordering of the graphite planes over the SiC substrate, but in a 1×1 form instead of the initial $6\sqrt{3}$ form where graphite is in direct connection with the underlying SiC planes. Actu-

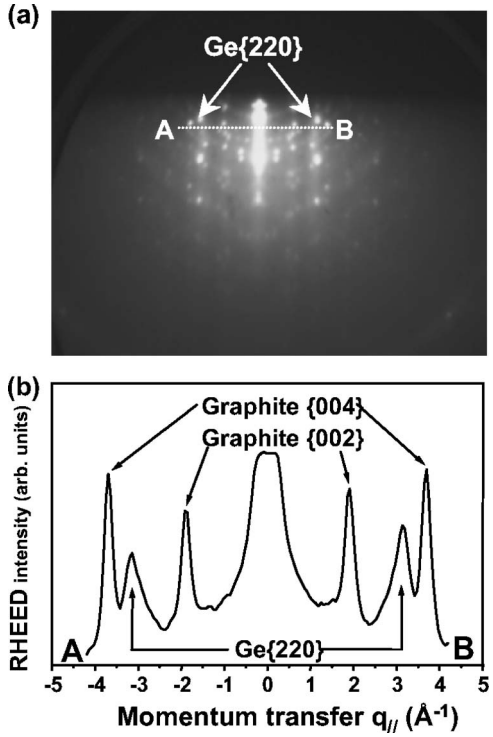

FIG. 2. Reminder of the complex RHEED spot-pattern of Fig. 1(d) after annealing 3 Ge ML at 600 °C (a) and corresponding intensity profile (b) traced along the A–B line on (a) and indicating the presence of both epitaxial Ge islands and "swollen" graphite clusters that will be visualized by AFM in Fig. 3(c).

ally, in this temperature regime, in addition to the 2D graphite restoration, we have also to notice the quasicomplete disappearance of the previous Ge-related spots. Surprisingly, this disappearance does not reflect a complete Ge sublimation from the substrate. As shown hereafter by chemical XPS analyses [Sec. III C], a significant Ge amount is persistently detected but is now lying in a 2D form under the reformed graphite planes instead of 3D islands. Ge has therefore been able to wet the SiC substrate, a fact explaining the restored overlying 2D graphite organization. The same chemical studies will show that Ge desorbs definitively and efficiently only above 1200 °C and will explain the progressive restoration of the initial $6\sqrt{3}$ RHEED (i),(j) and LEED (i′),(j′) patterns, only possible through the final Ge elimination.

In brief, the transitory stage of a rough graphitic organization between 600 and 800 °C is understood as the consequence of the Ge reorganization at the surface by an amazing 3D to 2D transition. We have of course checked that no graphite-sheet-dismantling takes place without Ge at the surface with the same annealing treatment. The observed behavior occurs only in the presence of Ge. The graphitic nanoobjects formed in this regime are not the topic of this work. Their precise determination will need further investigations, particularly by direct high-resolution transmission electron microscopy observations. In this study we especially intend to focus on the examination of the graphite/Ge/SiC heterostructure formed between 900 and 1100 °C.

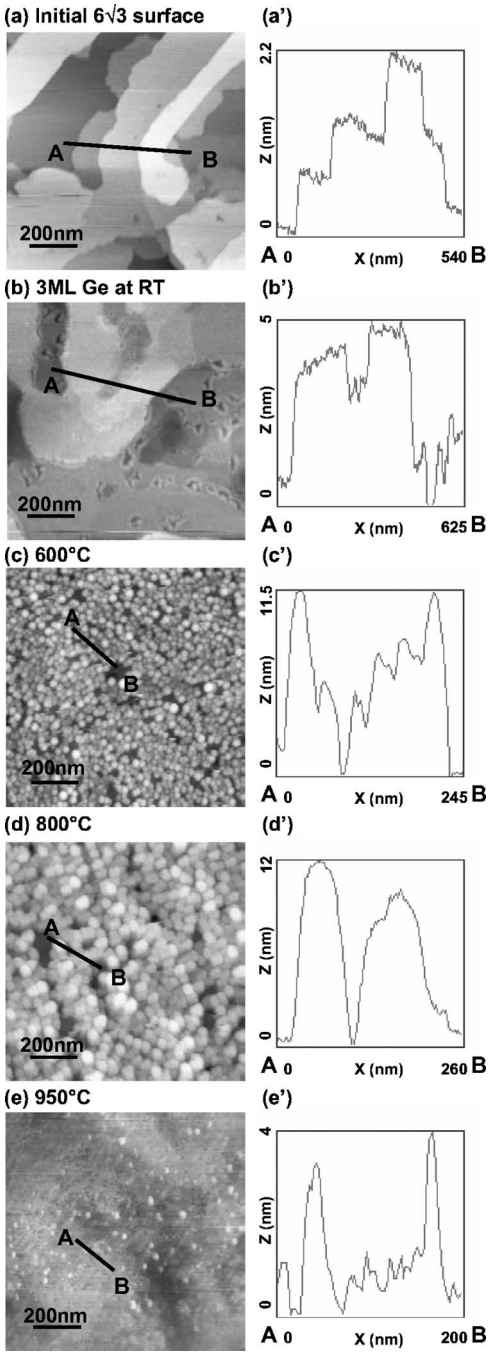

FIG. 3. Typical AFM (1 μm$\times$1 μm) images (a)–(e) and corresponding height profiles (a′)–(e′) of the initial 4H-SiC–$6\sqrt{3}$ substrate (a),(a′), covered by 3 Ge ML at RT (b),(b′) and showing the morphological modifications induced by post-annealing at different increasing temperatures (c)–(e) and (c′)–(e′).

B. AFM

Figure 3 summarizes the main morphological changes observed for some particular annealing steps. They essentially confirm the changes deduced from the electron diffraction examinations in the preceding section. The initial $6\sqrt{3}$ surface appears formed by large flat terraces delimited by a rather high density of steps (a),(a′), the overall roughness being a consequence of the Si desorption annealing at the

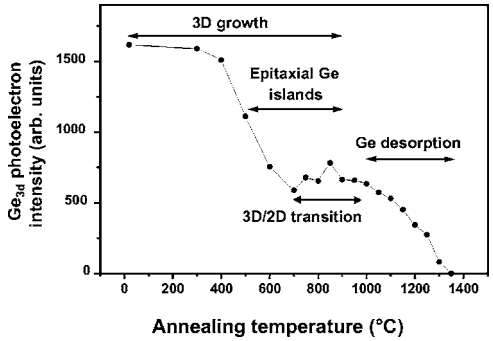

FIG. 4. Evolution as a function of 2 min post-annealing temperatures of the XPS Ge 3*d* core level intensity of 3 Ge ML deposited at RT on a graphitized $6\sqrt{3}-4$H-SiC surface. The present curve corresponds to grazing photoelectron detection ($\theta=60°$) but a similar behavior has been obtained at normal detection (curve not shown).

origin of this reconstruction. The 3 Ge ML deposit at RT adds some smooth protuberances, mainly in the depressions of the initial rough surface (b),(b′). They account for a nearly amorphous deposit of nonwetting Ge islands on the graphite planes as expected from the electron diffractions. The most spectacular change takes place in the 600–800 °C temperature range with the appearance of a very high density of clusters whose total volume is well beyond the nominal volume of the deposited Ge. This stage corresponds to the highly spotty RHEED patterns [Fig. 1(d) and 1(f)] that revealed both Ge- and graphite-related lattice parameters (Fig. 2). The large island density of the (c),(d) AFM images is therefore relevant to *both Ge and carbon clusters*. Even if the transitory formation of these carbon nano-objects is not the main topic of this study, it can be speculated that the significant volume increase seen by AFM could mainly be due to 2D graphite-plane deformations towards planes bended by the surface stress. At higher post-annealing temperatures [Fig. 3(e)], these high morphologies flatten out in accordance with the restoration of streaky RHEED patterns with 1×1-graphite signatures and the 3D–2D transition scheme for both Ge- and C-islands.

C. XPS chemical analyses

In Fig. 4 we first display the intensity evolution of the Ge 3*d* XPS core level throughout the complete temperature range scanned by the successive annealing steps. In addition to the checking of the Ge presence, this signal variation also provides indirect information about the morphology changes experienced by the Ge deposit. The initial intensity decrease, between 400 and 600 °C, is thus attributable on the one hand to the island coarsening seen by electron diffraction of the smoother and unordered 3 Ge ML coverage at RT into better formed epitaxial islands at higher temperature. On the other hand the intensity decrease may also account for the beginning of a partial desorption of Ge above the graphite planes. This stage is followed by an approximate intensity plateau above 600 °C correlated to the subsurface diffusion of the Ge under the graphite planes. The as-expected XPS Ge signal attenuation may be compensated by a signal increase due to the transfer of Ge matter from the islands to a wetting 2D layer. The definitive signal decrease, setting-on above 1100 °C, indicates the final desorption from the surface of the Ge part that was buried under the graphite, and that is completed at 1350 °C.

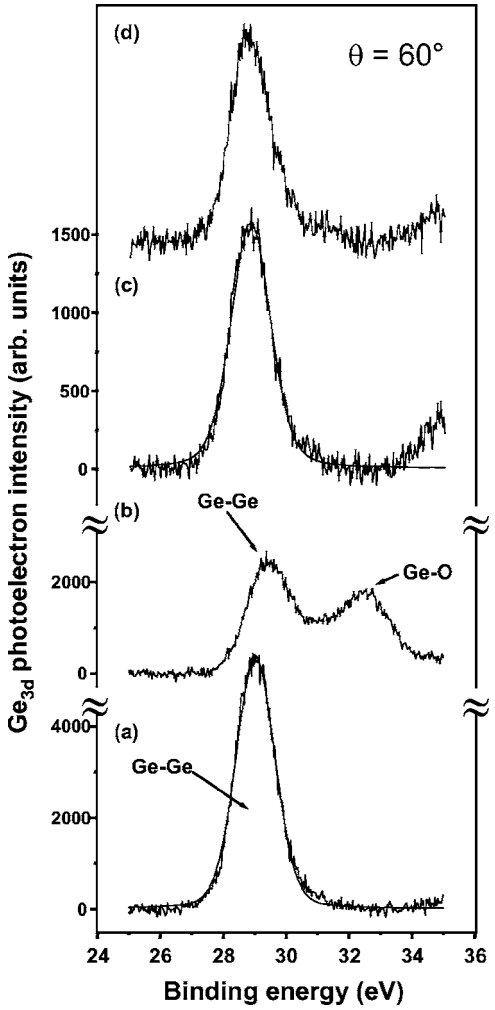

FIG. 5. Differentiated Ge-oxidation experiments done by the comparison of XPS Ge 3*d* core levels ($\theta=60°$) before and after air exposure of the nominal 3 Ge ML deposited at RT onto the graphitized reconstruction (a),(b) and the assumed buried Ge layer after post-annealing at 950 °C (c),(d). Ge may indeed be oxidized in the former case [(b) showing an oxide shifted component] and appears completely passivated in the latter one [absence of any significant oxide component in spectrum (d)] as expected for a buried Ge layer under the graphite planes.

A particularly convincing argument in favor of the subsurface diffusion-scenario of Ge atoms from the initial islands towards a bidimensional wetting layer under the graphite planes after annealing at 950 °C is provided by differentiated Ge behaviors against contamination. Figure 5 shows two pairs of Ge 3*d* spectra, each pair being relative to an oxidation experience by exposure to the atmospheric pressure. The former pair (a),(b) is relative to the initial RT Ge deposit and shows the Ge 3*d* spectra before (a) and after air exposure (b). An additional shifted component (~3 eV to-

wards higher binding energies) due to the native oxidation is clearly observed (b) whereas the unchanged component is related to Ge atoms-unaffected by the oxidation-inside the Ge islands. The latter pair (c),(d) concerns the same experiment but performed on a similar deposit annealed at 950 °C, a temperature at which the diffraction patterns and AFM data showed horizontal graphite sheets on rather flat surfaces. The absence of any significant oxidation feature after air exposure of this sample (d) can only be explained by an efficient passivation of the analyzed Ge amount. Moreover, with the absence of any Ge-related spots in the RHEED pattern at this temperature [Fig. 1(g)], a Ge δ-layer capped and passivated by a graphite top-plane seems to be a plausible explanation. An intercalation of a part of the initially deposited Ge between top-graphite planes and the SiC substrate is therefore reasonably admitted. As a remaining part of the Ge left at the surface may have desorbed during the thermal treatment up to 950 °C, the coverage of the intercalated Ge part is probably significantly lower than the nominal 3 ML deposit. The Ge 3*d* signal intensity analyzed at 950 °C (Fig. 4) is compatible with a coverage of about 1 ML.

The protective graphite capping, in addition to the previous passivation, also allows us to explain the very high final Ge desorption temperature (1350 °C) in comparison with similar Ge deposits on Si-rich SiC surfaces. In a previous systematic comparison[15] of Ge evolutions on three main (Si- or C-rich) SiC reconstructions, we observed -on SiC surfaces exempt of graphite- much lower desorption temperatures (950 and 1100 °C), more compatible with the melting point of Ge in standard conditions (938 °C). It is noteworthy here that the capping graphite layers are able to strongly delay this desorption temperature and to maintain a part of buried Ge atoms on the SiC surface up to 1300 °C.

Other additional argument may be put forward for strengthening the Ge 3D to 2D transition-scheme whose general driving forces must be a Ge repulsion for carbon and its tendency to react with the SiC substrate and to wet it under the graphite. On the one hand, the possibility for Ge to form 2D wetting layers on Si-terminated SiC surfaces has been largely demonstrated before (Refs. 15 and 16 and references therein). On the other hand, bulk-diffusion of Ge into the SiC matrix has to be completely excluded. In this case, as demonstrated by Diani *et al.*,[20] Ge atoms would preferentially substitute to Si ones and form heteropolar Ge-C bonds whose binding energy would differ from the homopolar Ge-Ge or Ge-Si bonds. Actually, during all morphological modifications experienced by the Ge atoms and described before, only *one* Ge 3*d* core level peak could be detected. It accounts for Ge-Ge bonds in the Ge islands observed in the low temperature range and probably to Ge-Si and lateral Ge-Ge bonds at the SiC surface in the wetting 2D form around 950 °C. The weak binding energy difference between these two homopolar forms remains below our experimental energy resolution. The absence of any Ge-C feature proves that Ge does not strongly bond with carbon, neither above the graphite planes after the low temperature deposit nor under them after its high temperature subsurface diffusion.

A subsidiary interrogation is whether the intercalated Ge layer presents any bidimensional ordering or not. As reminded in our introduction, the $6\sqrt{3}$ reconstruction is already assumed by some authors in the literature[3,6–8] to be formed by a submonolayer intercalation of an excess of Si in T_4 positions between truncated SiC(0001) and a graphite layer. Unfortunately, up to now no technique has been able to materialize this intercalation directly. We are facing similar experimental limitations to determine a possible Ge ordering beneath the graphite-layers. We have nevertheless demonstrated in previous reports that, on free surfaces (not capped by graphite), SiC(0001) may be terminated by a Ge layer (of about 1 ML) presenting a 4×4 ordering.[15,16] We can therefore only hypothesize similar arrangements for the intercalated Ge layer.

The XPD technique, performed here by polar angle recording of different core level intensities, is well known to provide valuable information about the local crystallographic environment of the selected atoms. This technique has previously been used on the SiC-system in references 7 and 20 and in some references therein. Applied for instance to Ge 3*d* core electrons with kinetic energies above 1 keV, the presence or not of angular forward scattering intensity modulations allows the discrimination of Ge atoms either aligned in atomic rows of organized islands or in a surface 2D layer without any forward focusing effect, respectively. In the present case we effectively observe a forward scattering peak for the Ge 3*d* level in the surface normal direction ($\theta=0°$) in the 500–800 °C temperature range, i.e., as long as ordered Ge islands are observable by electron diffraction or AFM. This intensity modulation at polar angle $\theta=0°$ completely vanishes near 950 °C, a fact that reflects a now prevailing 2D organization of the analyzed Ge atoms.

XPD may also be used to discriminate between the SiC bulk- and surface-contributions in the Si 2*p* or C 1*s* core levels. Let us label as B_1 such former bulk-components recorded for instance on the initial $6\sqrt{3}$ surface and characteristic of the bulk-SiC crystallography that is not recalled here. In the present case of a graphitized C-rich surface, the Si 2*p* peak is only composed of a unique B_1 bulk component of Si atoms in their tetrahedral environment in the SiC matrix.[7] The corresponding XPD angular distributions along different crystallographic azimuths are therefore the signatures of the hexagonal structures of SiC already reviewed in the literature (references 7 and 20 and references therein). For the C 1*s* peak the situation is more complex since it contains a similar bulk-contribution added to surface components due to the presence of the graphite over-layer.[4,5,7] Only the decomposed C 1*s* bulk-component shows angular modulations characteristic of the probed crystal in this case. No observation of forward focusing modulation is expected on the C 1*s* surface component relative to the bidimensional graphite layers.

D. Surface band bending derived from XPS data

We now intend to describe surprising and spectacular trends occurring on these B_1 bulk-components concomitantly to the Ge subsurface reorganizations, i.e., between 600 and 1350 °C. To simplify, we only display in Fig. 6 the modifications on the Si 2*p* B_1 signal, but parallel behaviors are observed on the deconvoluted C 1*s* bulk-component. As a function of increasing annealing temperature, above 600 °C,

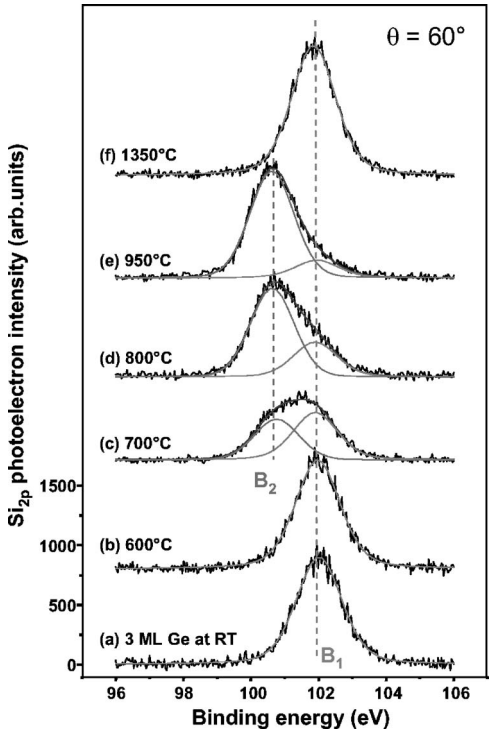

FIG. 6. Typical XPS Si $2p$ core level evolutions with post-annealing temperature. They show a pairing of the SiC bulk-component in two binding energy shifted subcomponents B_1 and B_2 exchanging their intensities as a function of annealing temperature.

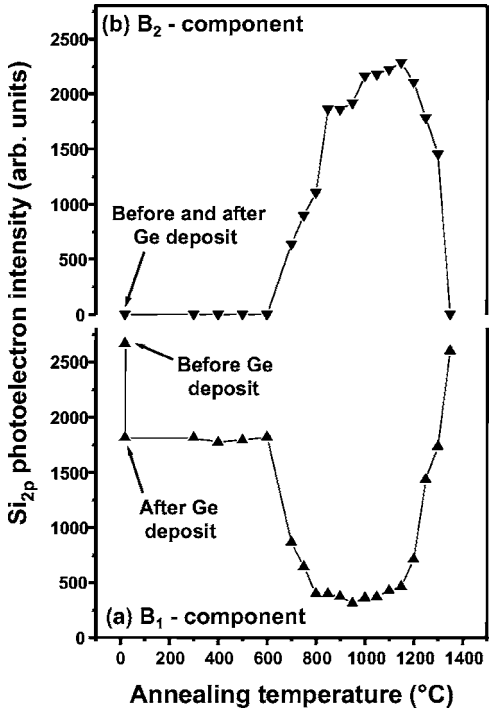

FIG. 7. Compared XPS Si $2p$ intensity evolutions of the B_1 and B_2 components as a function of post-annealing temperatures. The observed component exchange, deduced from spectra like those of Fig. 6, begins at 600 °C, reaches a maximum around 900–1100 °C and disappears with the complete Ge desorption (see Fig. 4).

the B_1 component begins to exchange its intensity with a binding energy shifted component labeled B_2 (b), (c). The latter reaches its maximum near 950 °C (e). Afterwards a B_2 re-decrease is accompanied by a concomitant progressive return of B_1 which is completely restored at 1350 °C (f). We have checked that both B_1 and B_2 components exhibit completely identical XPD angular distributions (not shown). This fact clearly proves that both signals originate from similar bulk atoms, i.e., in the same crystallographic and chemical SiC environments. As a consequence, the binding energy shift of about 1.2 eV that differentiates these components is not of chemical origin but must rather be due to different surface potential conditions inducing different space charges or band bendings in two different types of surface areas. The respective parts of these surface areas evolving with temperature should therefore be simply proportional to the intensities of the B_1 and B_2 signals.

Let us therefore connect the temperature domain of these bulk-signal energy-exchanges with that of the Ge morphological story. We first remind that a drastic Ge change begins at 600 °C with a sub-surface diffusion under the graphite planes that generates carbon-clusters [evolution (b)–(c)]. Near 950 °C, a mostly complete graphite/Ge/SiC termination denoting a best Ge wetting and reactivity with the SiC substrate is proposed to occur under graphite planes in 1×1 registry with the substrate (e). The Ge story finishes at 1350 °C with its complete desorption (f). The correlations and temperature interplays between the previously described spectroscopic modifications on the B_1 and B_2 bulk features and the morphological evolutions deduced from the electron diffractions and the chemical Ge $3d$ analyses are particularly striking.

The B_1–B_2 core level pairing is best summarized in Fig. 7 which sums up the complete intensity exchanges and shows the complementary nature of these components all along the annealing cycles, with extremes around 900–1000 °C. The nearly constant B_1+B_2 intensity sum accounts for the bulk-analysis of the whole surface area. Each separated B_1 (a) or B_2 (b) intensity reflects the analysis of the complementary surface areas exchanging during the thermal treatment of the SiC surface, i.e., either covered by only graphite (or graphite/SiC structure for B_1) or by Ge covered by graphite (or graphite/Ge/SiC structure for B_2), respectively. The intensity evolutions of Figs. 6 and 7 appear thus easily explainable. Similar binding energy modifications of SiC bulklevels in relation with surface graphite plane evolutions have already been mentioned in the past by Johansson *et al.*[4,5] (dimly attributed to "Fermi level pinning differences") or by Simon.[21]

In the present case of 3 Ge ML deposition, we can also notice that a nearly complete conversion of the B_1 and B_2 intensities is possible (Fig. 7). This completion in the intensity conversion signifies that the Ge amount deposited in the present case is probably sufficient to convert the whole surface into a graphite/Ge/SiC termination. In the course of a previous study, with only 1 ML Ge deposition,[15] the general Ge $3d$ behavior was also similar to that given in the present paper in Fig. 4. Moreover, we qualitatively observed the same subsurface Ge diffusion phenomena on the $6\sqrt{3}$ reconstruction in the high temperature regime. Not well under-

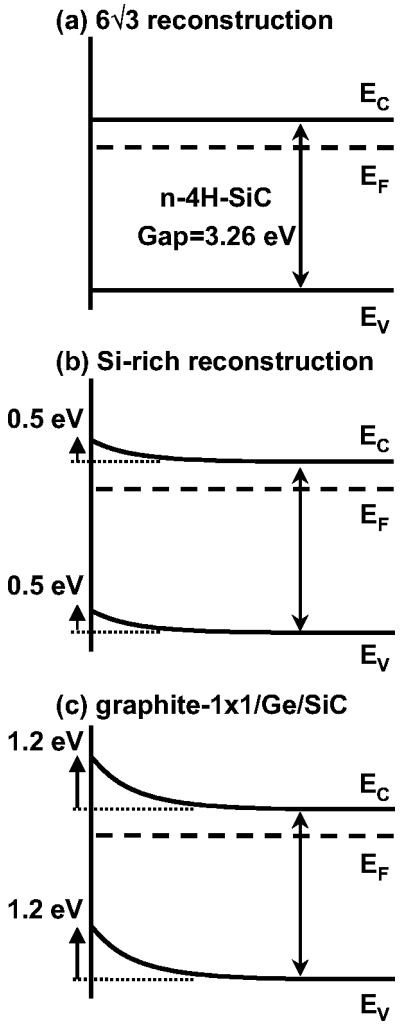

FIG. 8. Attempted band bending interpretation of the observed spectroscopic B_1 (a) and B_2 (c) modifications of the bulk core levels that would account for two different surface terminations (B_1 = graphite capping SiC and B_2 = graphite with intercalated Ge on SiC, respectively) whose respective surface areas vary with post-annealing temperature. Schematization (b) accounts for a lower binding energy shift observed for Si enrichment of the SiC surface, causing a lower band bending, intermediate between the B_1 and B_2 situations.

stood at that time, these phenomena had not been addressed in Ref. 15. Compared quantitatively to the present situation (3 ML), they differed by the fact that the conversion of the B_1 component into the B_2 one was much less complete than that shown in Fig. 6 or 7. This agrees with an incomplete surface covering of 2D Ge under the graphite planes, in accordance with a lower deposited amount of Ge. Actually, the amount of the residual Ge in B_2 situation under the graphite planes depends essentially -of course- on the initial Ge amount but also on the degree of graphitization of the initial surface. Using other independent AFM experiments (not shown here for space constraints) on less C-rich surfaces i.e., exhibiting a mixture of $\sqrt{3}$ and $6\sqrt{3}$ reconstructions, we have checked that the typical island swelling above 600° only appeared on restricted areas that certainly corresponded to those covered by graphite.

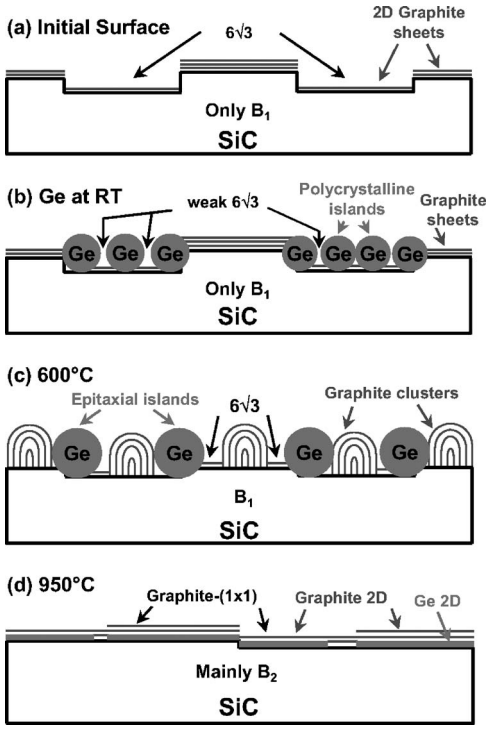

FIG. 9. Explanatory schematization of the rather complex Ge story as it may be deduced from the collected information. Four key-situations are represented corresponding from (a) to (d) to: (a) the initial graphitized surface, (b) after a RT 3 Ge ML deposit, (c) after post-annealing at 600 °C where Ge begins to react with the substrate and swells the graphite planes, and (d) after 950 °C annealing where graphite planes are bidimensionally reorganized again over a 2D Ge wetting layer. The graphite/Ge/SiC heterostructure occasions a B_2 binding energy shift in the bulk due to a band bending given in Fig. 8.

The previous B_1 and B_2 assignments allow us to sketch (Fig. 8) possible band bending modifications compatible with the *n*-doped SiC substrates used in this work, the respective surface status and the photoemission binding energy shift-observations. The coherence of these data implies rather flat bands for the B_1 situation (graphite upon SiC), compatible with weak or negligible charge transfers between graphite and SiC (8a), as previously mentioned by Forbeaux *et al.*[6,8] Strong electron depletion should therefore be deduced in the B_2 situation for the intercalated Ge layer between graphite and SiC (8c). The corresponding analyzed surface region of SiC experiences indeed a 1.2 eV shift towards lower bulk-binding energies with respect to the B_1 situation making the occupied bands come closer to the Fermi level in the surface region of XPS analysis. An upward band bending (8c) should therefore be the reason of the B_2 energy shift. We can notice that a similar upward band bending has also been observed in the elaboration of Schottky barriers using ultrathin nickel metallic coverages on SiC(0001)[22,23] or Cu deposits on SiC(000-1).[24] Moreover, in the work of Hoshino *et al.*[22] a production of C-clusters like ours (as a byproduct of the Ni-reaction with the SiC substrate) has been shown by AFM in conjunction with an upward band bending of the bulk Si 2*p* component.

The origin of the strong surface charge transfer, that must be associated to the Ge-induced band bending, is still unclear. At this stage, we can nevertheless notice that weaker energy shifts (also towards lower binding energies or upward band bending) have been observed by Johansson *et al.*[5] (0.7 eV) and us (only 0.5 eV) for Si-enriched SiC surfaces (3×3 or $\sqrt{3}$) with respect to the B_1 value for a $6\sqrt{3}$ surface. They are compatible with a less consequent upward band bending [Fig. 8(b)] than for B_2 (1.2 eV) related to a Ge covering [Fig. 8(c)]. Covering an *n*-doped SiC surface with Ge or Si seems therefore to induce a more or less important negative charge at the surface neutralized by a positive depletion charge in the SiC substrate. Depending on Ni coverage, binding energy shifts between 0.3 and 1.0 eV have been reported on *n*-type 6H-SiC surfaces by Hoshino *et al.*[22] Regarding the charge transfer, Ge seems therefore to act similarly to metallic elements.

As a final but edifying remark, we have to emphasize that all the previously described phenomena are certainly largely favored by a post-annealing procedure of RT Ge-deposition on graphitized SiC surfaces. Actually, direct high temperature Ge deposition would lead to lower sticking on graphite and significantly hinder the Ge uptake at the surface. Subsurface diffusion of Ge would *-a fortiori-* be impeded. The growth procedure we employed here, i.e., RT deposition followed by post-annealing, is therefore an essential ingredient to obtain the observed heterostructure and the associated Schottky-barrier-like band bending more easily. It is noteworthy that Hoshino *et al.*[22] used the same procedure to get similar phenomena with Ni.

IV. CONCLUSION

Figure 9 shows a schematization of the complex Ge transformations induced by the post-annealing treatment and deduced from the collected information. After a schematized view of the initial graphitized surface (a), and subsequent RT Ge 3D deposit over the $6\sqrt{3}$ surface (b), post-annealing at 600 °C marks the beginning of the Ge reaction with the substrate. Ge islands are formed in epitaxial registry with SiC with a concomitant and transitory graphite-plane swelling (c) seen as carbon-clusters by RHEED or AFM. Further annealing allows Ge to undergo a surprising island dismantling in an unusual 3D–2D transition by which it wets the SiC substrate under the graphite bi-dimensionally restored as well. This smoothed re-ordering of both Ge and graphite is completed at 950 °C (d) as reflected by graphite-1×1 RHEED and LEED patterns. The as-achieved graphite/Ge/SiC structure also causes a spectacular binding energy shift ($\sim$1.2 eV) in the XPS bulk levels due to a band bending effect. The intercalation of an approximate δ-monolayer of Ge between the graphite planes and the SiC surface is therefore made possible and acts as a Schottky barrier on the substrate. The graphite capping passivates the inserted Ge-layer against air-contamination and delays the Ge-desorption during further postannealing. Complete band bending suppression, accompanied by a relevant restoration of the initial $6\sqrt{3}$ reconstruction of graphite in direct registry with SiC (i.e., without Ge), only occurs after complete Ge desorption at a temperature as high as 1350 °C.

ACKNOWLEDGMENTS

The authors would like to thank A. Galliano (ICSI, Mulhouse) for assistance in the AFM measurements and L. Simon (LPSE, Mulhouse) for communication of unpublished results.

*Corresponding author. Present address: LPSE, CNRS UMR 7014, 4, rue des Frères Lumière, 68093 Mulhouse Cedex, France. Electronic address: l.kubler@uha.fr

[1] A. J. Van Bommel, J. E. Crombeen, and A. Van Tooren, Surf. Sci. **48**, 463 (1975).
[2] C. S. Chang, I. S. T. Tsong, Y. C. Wang, and R. F. Davis, Surf. Sci. **256**, 354 (1991); M.-H. Tsai, C. S. Chang, J. D. Dow, and I. S. T. Tsong, Phys. Rev. B **45**, 1327 (1992).
[3] J. E. Northrup and J. Neugebauer, Phys. Rev. B **52**, R17001 (1995).
[4] L. I. Johansson, F. Owman, and P. Martensson, Phys. Rev. B **53**, 13793 (1996).
[5] L. I. Johansson, F. Owman, and P. Martensson, Surf. Sci. **360**, L483 (1996).
[6] I. Forbeaux, J.-M. Themlin, and J.-M. Debever, Phys. Rev. B **58**, 16396 (1998).
[7] L. Simon, J. L. Bischoff, and L. Kubler, Phys. Rev. B **60**, 11653 (1999).
[8] I. Forbeaux, J.-M. Themlin, A. Charrier, F. Thibaudau, and J.-M. Debever, Appl. Surf. Sci. **162**, 406 (2000).
[9] X. N. Xie, H. Q. Wang, A. T. S. Wee, and K. P. Loh, Surf. Sci. **478**, 57 (2001).
[10] G. Hess, A. Bauer, J. Kräusslich, A. Fissel, B. Schröter, W. Richter, N. Schell, W. Matz, and K. Goetz, Thin Solid Films **380**, 86 (2000).
[11] B. Schröter, K. Komlev, U. Kaiser, G. Hess, G. Kipshidze, and W. Richter, Mater. Sci. Forum **353**, 247 (2001).
[12] B. Schröter, K. Komlev, and W. Richter, Mater. Sci. Eng., B **88**, 259 (2002).
[13] P. Weih, Th. Stauden, and J. Pezoldt, Mater. Sci. Forum **389**, 725 (2002).
[14] C. Calmes, V. Le Thanh, D. Bouchier, S. E. Saddow, V. Yam, D. Débarre, R. Laval, and C. Clerc, Mater. Res. Soc. Symp. Proc. **742**, 143 (2003).
[15] K. Aït-Mansour, L. Kubler, D. Dentel, J. L. Bischoff, M. Diani, and G. Feuillet, Surf. Sci. **546**, 1 (2003).
[16] K. Aït-Mansour, L. Kubler, M. Diani, D. Dentel, J. L. Bischoff, L. Simon, J. C. Peruchetti, and A. Galliano, Surf. Sci. **565**, 57 (2004).
[17] K. Aït-Mansour, D. Dentel, J. L. Bischoff, L. Kubler, M. Diani, A. Barski, M. Derivaz, and P. Noé, Physica E (Amsterdam) **23**, 428 (2004).
[18] K. Aït-Mansour, D. Dentel, L. Kubler, M. Diani, J. L. Bischoff, and D. Bolmont, Appl. Surf. Sci. **241**, 403 (2005).

[19] K. Aït-Mansour, D. Dentel, L. Kubler, M. Diani, J. L. Bischoff, and A. Galliano, J. Cryst. Growth (unpublished).
[20] M. Diani, L. Kubler, L. Simon, D. Aubel, I. Matko, and B. Chenevier, Phys. Rev. B **67**, 125316 (2003).
[21] L. Simon (private communication).
[22] Y. Hoshino, O. Kitamura, T. Nakada, and Y. Kido, Surf. Sci. **539**, 14 (2003).
[23] S. Y. Han and J. L. Lee, Appl. Phys. Lett. **84**, 538 (2004).
[24] I. Dontas, S. Ladas, and S. Kennou, Diamond Relat. Mater. **12**, 1209 (2003).